ISTITUTO NAZIONALE DI FISICA NUCLEARE
Laboratori Nazionali di Frascati

LNF-82/3(R)
27 Gennaio 1982

R. Del Fabbro and G. P. Murtas: HIGH RATE LUMINOSITY MONITOR IN THE LEP MINI-BETA SHORT INSERTION

Servizio Documentazione
dei Laboratori Nazionali di Frascati
Cas. Postale 13 - Frascati (Roma)

INFN - Laboratori Nazionali di Frascati
Servizio Documentazione

LNF-82/3(R)
27 Gennaio 1982

HIGH RATE LUMINOSITY MONITOR IN THE LEP MINI-BETA SHORT INSERTION

R. Del Fabbro
INFN, Sezione di Pisa

and

G. P. Murtas
INFN, Laboratori Nazionali di Frascati, and Istituto di Fisica, Facoltà di Ingegneria dell'Università di Napoli

ABSTRACT.

The real possibility is investigated of setting up a high rate luminosity monitor in a mini-beta short insertion of LEP.

Since angles as small as possible have to be reached by the detecting system, electrons detectors have been considered both behind and inside the low-beta quadrupole looking at electrons of Bhabha scattering events.

Results show the feasibility of a high rate monitor, and expected Bhabha rates are given at various LEP energies.

The relevance of the synchrotron radiation background has been extensively studied and found to be negligible for a total energy absorption counter.

A rough investigation has also been paid to the real beam effects and to the off-momentum particles background.

1. - INTRODUCTION.

In the e^+e^- storage rings the continuous luminosity monitor has been estensively used in the past and it is used today, where it is possible, in the present functioning storage ring.

The high rate luminosity monitor consists of a pair of detectors symmetrically located around the crossing point loocking at a very small angle recoil electrons of the Bhabha scattering.

Such a continuous monitor is not, in general, a very accurate instrument (not less than 10%) and usually the integrated luminosity collected by an experimental apparatus in the running time is evaluated by the large angle Bhabha events detected by the central detector with an accuracy of the order of the 1%. However the continuous luminosity monitor is useful for a quick knowledge of the beam luminosity and for a continuous check of the machine performance.

The recent proposal[1] presented at the "General Meeting on LEP" of reducing the short insertion length at $\pm$ 3.5 m gets as consequence that the minimum polar angle one can reach is of the order of 30 mrad. This value is much too large for a high rate luminosity monitor, taking into account the $1/\theta^4$ dependence of the Bhabha $d\sigma/d\cos\theta$ differential cross section. For instance a detector in front to the quadrupole QS1, covering an angular range from 30 to 120 mrad, can collect only 111 nb at 50 GeV.

The aim of this paper is to investigate on the possibility of setting up a high rate monitor located behind or inside the QS1 quadrupole in order to reach polar angles as small as possible. Results on this subject are reported in Section 2, where the simple case is discussed of an electron detector located behind the QS1 quadrupole very close to the beam pipe (16 cm in diameter). In Section 3 the case of a beam pipe reduced in diameter to 10 cm is discussed. The pipe reduction in the quadrupole QS1 region allows of extending the electron detector inside the quadrupole using the gap between the pipe and the quadrupole wall. Undoubtedly this possibility, if realistic, is very appealing not only for the luminometer improvement, but also for the implications on the two photon physics. In fact for the luminometer a large gain is already achieved through a nearer beam distance, whereas for the two photon physics experimentation one can cover a contiguous angular range from large to very small angles. Following our line of interest on the two photon physics experimentation at LEP[2] a paper on this subject is now in preparation.

Since a strong argument against such an interesting possibility could be the danger of high synchrotron radiation falling on the electron detector, in Section 4 we have studied the effects of the synchrotron radiation emitted in the horizontal plane by the electron beam passing through the quadrupoles QS1 and QS2. In Section 5 some rough calculations results are reported on the Bhabha rate variations due to the real beam effects. Finally in Section 6 effects of the beam-gas background on the monitor have been discussed.

2 - THE CASE (A) OF AN ELECTRON DETECTOR BEHIND THE QS1 QUADRUPOLE.

The lattice of the "reduced short insertion" as recently proposed[1] at "General Meeting on LEP" appears as it is shown in the lay-out of Fig. 1a. The quadrupoles QS1 and the doublet QS2' and QS2" are closer to the crossing point with respect to the Pink Book design. The QS1 is a superconducting quadrupole 3.5 m long and of quadrupolar constant $K = 0.1188$ m^{-2}. The doublet QS2 are standard quadrupoles 2 m long of quadrupolar constant $K = 0.042$ m^{-2}. In particular QS1 is a cylinder of 60 cm in external diameter and the diameter of its internal aperture is 17 cm fitting suitably the beam pipe diameter of 16 cm.

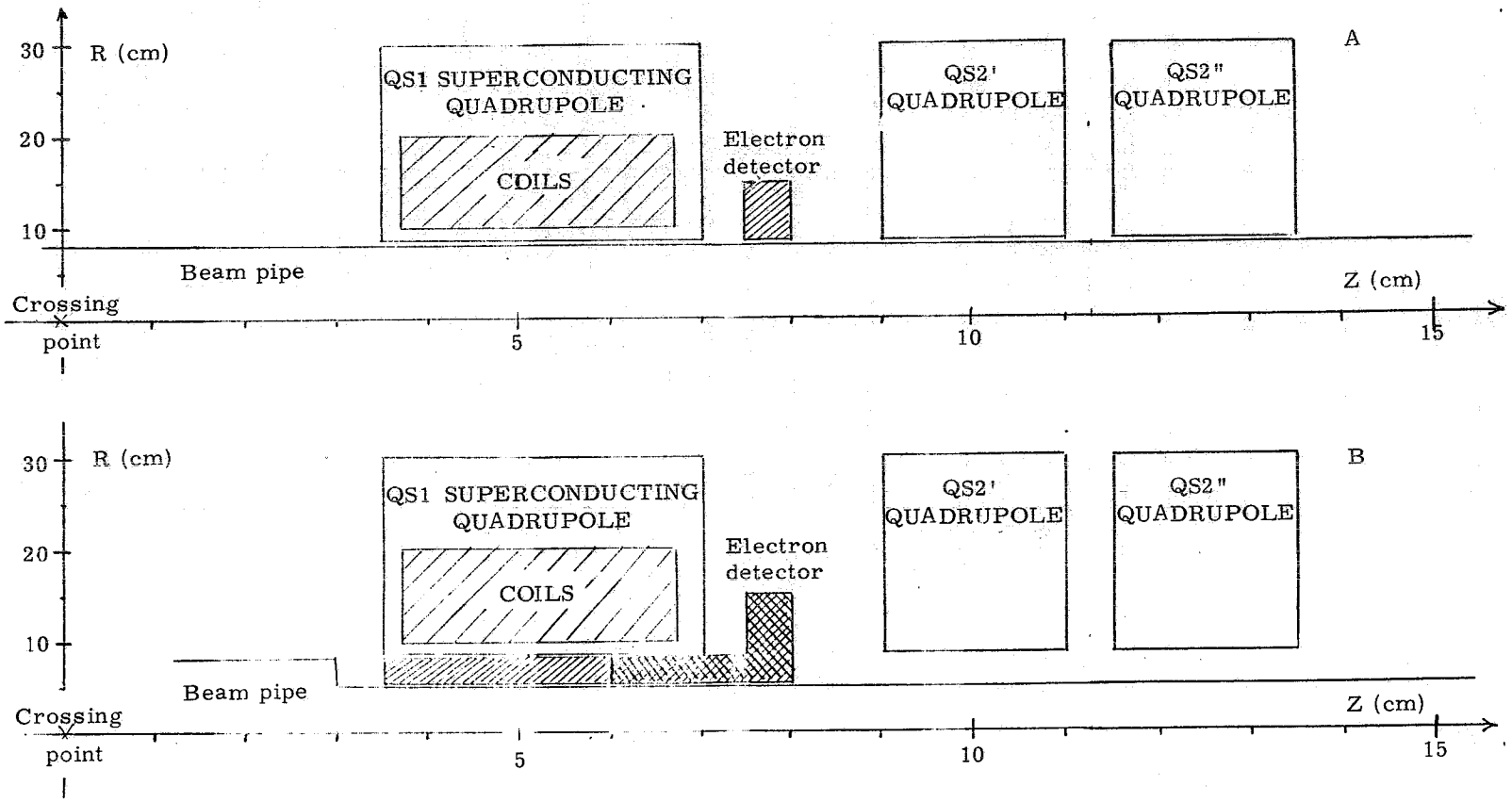

FIG. 1 - Lay-out of the mini-beta equiped short insertion. A) Electron detector behind the QS1 quadrupole close to the beam pipe of 16 cm diameter. B) Electron detector behind and inside the QS1 quadrupole around the beam pipe of 10 cm diameter.

We have studied the electron trajectories through this lattice as function of θ and ϕ, the electron polar and azimuthal angles. The electron is supposed to be emitted in the crossing point at an energy $X_e = 1$ (in beam energy unit).

Let us consider the two following conditions :

i) $y < 9.7$ cm when $3.5 \leq z \leq 6.7$ m

ii) $y \geq 9$ cm when $z = 8$ m

where y is the distance of the electron trajectory from the machine axis and z is the beam line coordinate, the origin being in the crossing point.

The former condition requires that the electron doesn't cross heavy material passing through the quadrupole QS1. In fact in the present design of the superconducting quadrupole the layer between 8.5 cm and 9.7 cm consists of relatively thin material. Behind 9.7 cm some layers of steel are encountered as it is shown in Fig. 1, where the dashed area of the quadrupole indicates the region where the coils are located. The latter condition requires that the electron trajectory behind the quadrupole QS1 be at a sufficient distance from the beam centre in order to cross the electron detector placed very close to the beam pipe.

The region of the plane (θ, ϕ) where both above conditions are satisfied is indicated by the dashed line of Fig. 2. Basically the region is sized by two bounding curves : the first one limiting the small θ angles is fixed by the condition ii), the second one limiting the large angles by the condition i). In Fig. 2 is shown only a quadrant of the whole ϕ angular range, but it is quite clear that the symmetry of the quadrupolar field around the radial and vertical axes allows to know also the other regions of the same shape symmetrically disposed in the other quadrant.

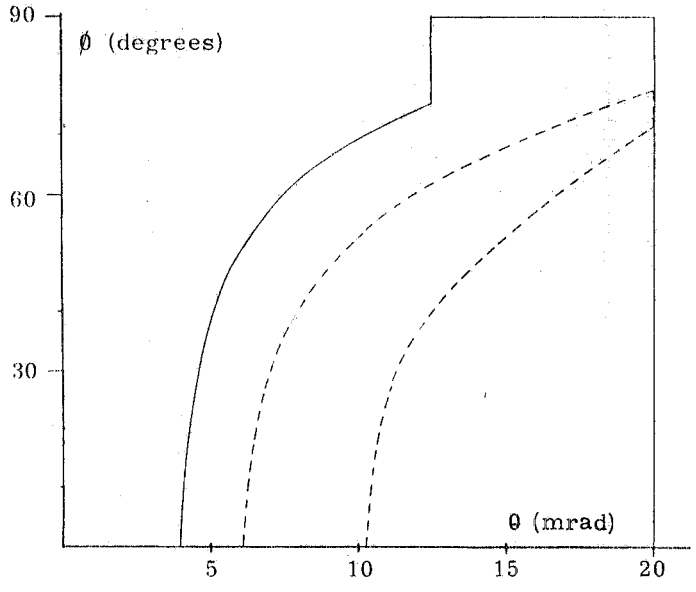

FIG. 2 - Regions of acceptance in the plane θ, ϕ. Dashed lines (full lines) are relative to the case Λ (B).

Since we are interested to detect the recoil electrons in the region behind the QS1 quadrupole, in Figg. 3a and 3b are reported the regions confined by dashed lines indicating the cross sections of the detectable trajectories at longitudinal coordinates of $z = 7$ m and $z = 8$ m respectively.

By the lowering of the iso-ϕ lines of 30 and 60 degrees shown in the Figg. 3a and 3b one can realize how the defocalizing action of the quadrupole QS1 leads all the detectable trajectories in the radial direction. So one can deduce that the electron detector must be disposed horizontally very close to the beam pipe and it can be

quite small in size: of the order of tenth centimeters. In Fig. 4 the transverse shape of such a detector is sketched.

Actually such a detector can be composed of four elements, for instance corresponding to the four quadrants. In this way the Bhabha events can be detected requiring the coincidence of opposite quadrants between two detectors located on the left and right side of the crossing point.

The rate of the Bhabha scattering events can be given as follows:

$$N_{Bh} = \mathcal{L}_{e^+e^-} 2\pi \int_{-1}^{+1} d\cos\theta \left(\frac{d\sigma}{d\cos\theta}\right)_B f(\theta) \qquad (sec^{-1}) \qquad (1)$$

where $\mathcal{L}_{e^+e^-}$ is the beam luminosity and $f(\theta)$ is the fraction of the azimuthal angle one can detect at each polar angle θ.

Such a function $f(\theta)$ can be easily got from the detectable region of Fig. 2 and it is plotted versus θ in Fig. 5 (curve A).

The $(d\sigma/d\cos\theta)_{Bh}$ is the Bhabha scattering differential cross section of which in the considered angular range the leading term is a good approximation:

$$\left(\frac{d\sigma}{d\cos\theta}\right)_{Bh} \cong \frac{4\alpha^2}{E_b^2 \theta^4} \; . \qquad (2)$$

Results of the integral in the expression (1) are reported in Table I as case "A" for different beam energies, corresponding to different realization phases of the LEP storage ring[3].

TABLE I - Bhabha scattering integrated cross section.

LEP Phase	E_{beam} (GeV)	$30 \leq \theta \leq 120$ mrad (nb)	A $6 \leq \theta \leq 20$ mrad (nb)	B $4 \leq \theta \leq 20$ mrad (nb)
I	50	111	841	2951
III	86	38	285	999
V	130	17	125	437

3. - THE CASE (B) RELATED TO THE BEAM PIPE REDUCTION.

Results of Section 2 shown in Table I indicate that by a simple electron detector located behind the QS1 quadrupole is possible to achieve about an order of magnitude in rate with respect to a detector in front to QS1. That means that a high rate luminosity monitor in the reduced short insertion is actually feasible.

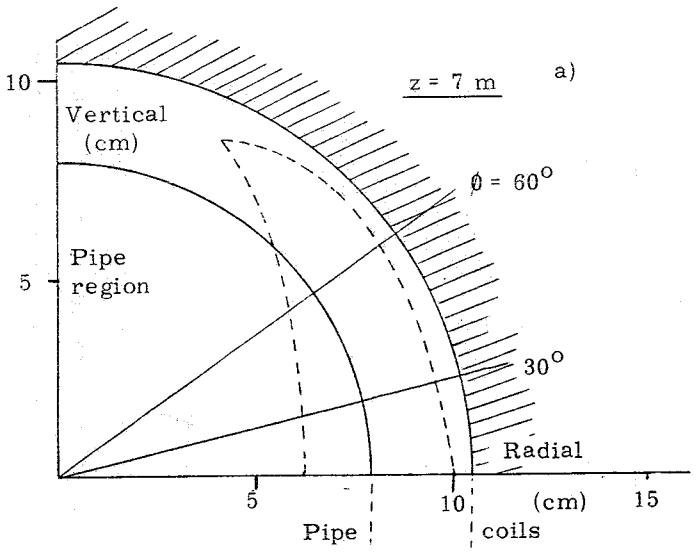

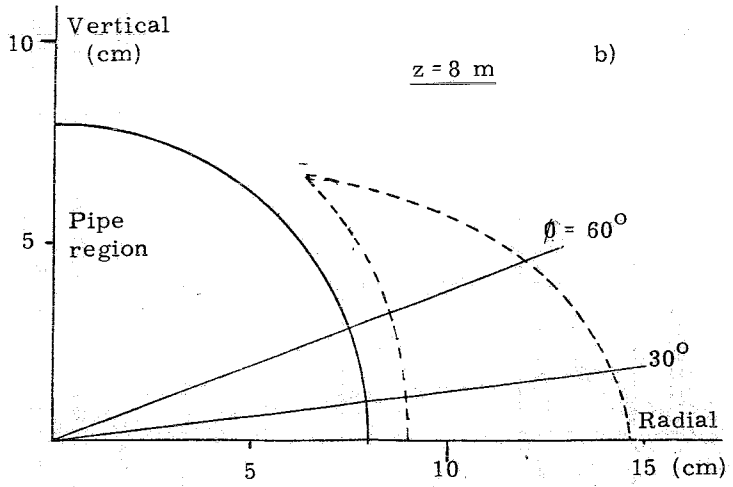

FIG. 3 - Cross-sections of the detectable trajectory fraction by dashed lines. a) Cross-section by a transverse plane at z = 7 m. b) Cross-section by a transverse plane at z = 8 m.

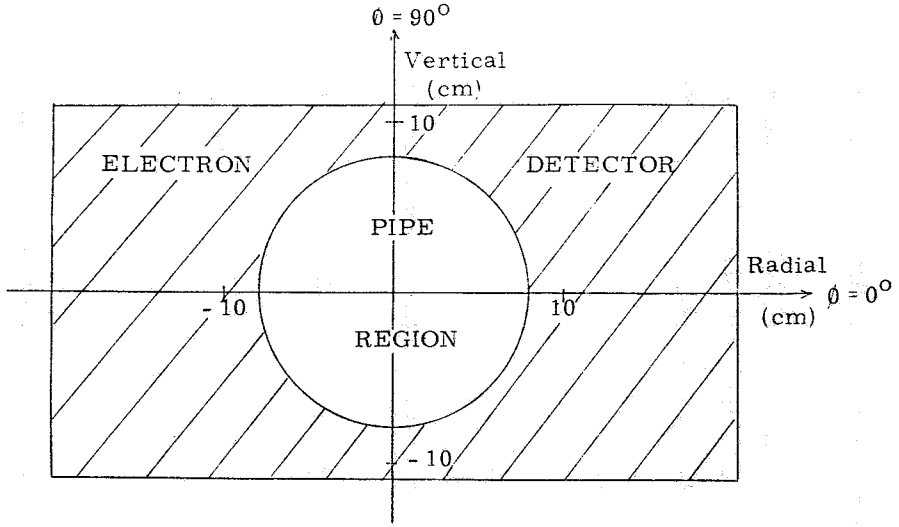

FIG. 4 - Trasverse view of a possible electron detector located behind the QS1 quadrupole.

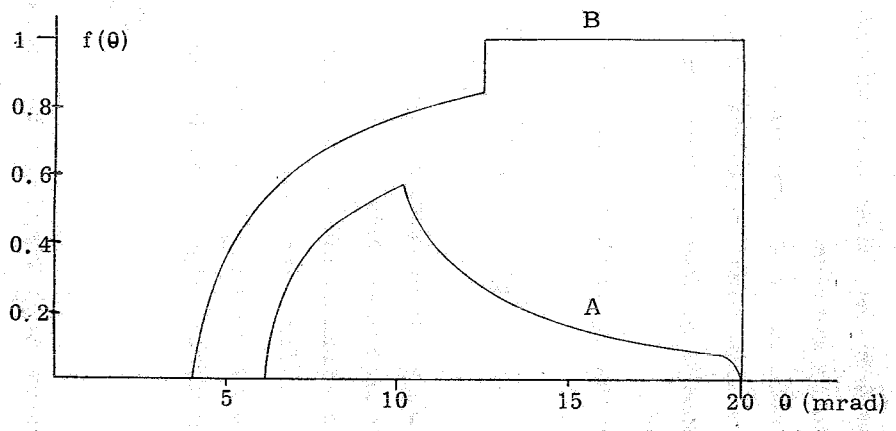

FIG. 5 - Detectable trajectory fraction spectra relative to the case A and B respectively.

However the Bhabha rate can be further increased if an electron detector could be located inside the quadrupole QS1. That can be possible with a beam pipe of 10 cm in diameter in the quadrupole region. In this way one could use 3.5 cm of gap between the pipe and the internal quadrupole wall, housing an total energy absorption electron detector covering the whole azimuthal angle (see the Fig. 1B).

For the Bhabha scattering monitor the counter length inside the pipe could be of the order of one meter (see the grated part of the detector in Fig. 1B, however we judge to be useful covering the whole quadrupole length by a detector mainly dedicated to the two photon physics study and to measurements of energy released at very small angles.

It is well known that the pipe size around the crossing point depends heavily on the background configuration, mainly the synchrotron radiation. That is why in the next Section we have studied the synchrotron radiation background in order to check the feasibility of this solution, which seems very promising not only for some improvement of a high rate monitor, but also for some interesting implications for the two photon physics experimentation.

In this Section we have repeated the calculation of Section 2 dropping the condition i) and lowering the minimum distance of the electron detector from 9 cm to 6 cm in the condition ii). All the trajectories are bent toward the quadrupole wall in the radial direction. Some trajectories hit the internal detector with a rather small grazing angle: from 20 to 60 mrad depending on the electron polar angle.

In Fig. 2 the full line in the plane (θ, ϕ) indicates the detectable region in this case, one can see how the accepted region is greatly expanded with respect to the previous case (dashed line). In fact the lack of the condition i) extends fully the range of the detectable region toward the large angles.

The spatial evolution of the trajectories is represented in Fig. 6 through five transverse cross sections: at beginning, at 1/3, 2/3 of the length, at the end of the quadrupole and the last behind the quadrupole itself. In Fig. 6a the dark area represents the region of the detectable trajectories with $\theta < 14.3$ mrad. In order to follow better the trajectories evolution inside the quadrupole the iso-θ curves (circles) at $\theta = 7$ mrad and 10 mrad and the iso-ϕ lines at 30, 60 and 80 degrees are indicated. In the successive pictures of Fig. 6b, c, d and e one can see how the iso-θ curves change from circular to elliptical and the iso-ϕ lines are lowered down more and more. The area representing the detectable trajectories in the pipe region is progressively reduced and in Fig. 6d represents the trajectories coming out from the quadrupole QS1.

In Fig. 5 the corresponding function $f(\theta)$ is described by the curve "B" and therefore the integrated Bhabha cross section can be evaluated. Results are shown in Table I as case "B".

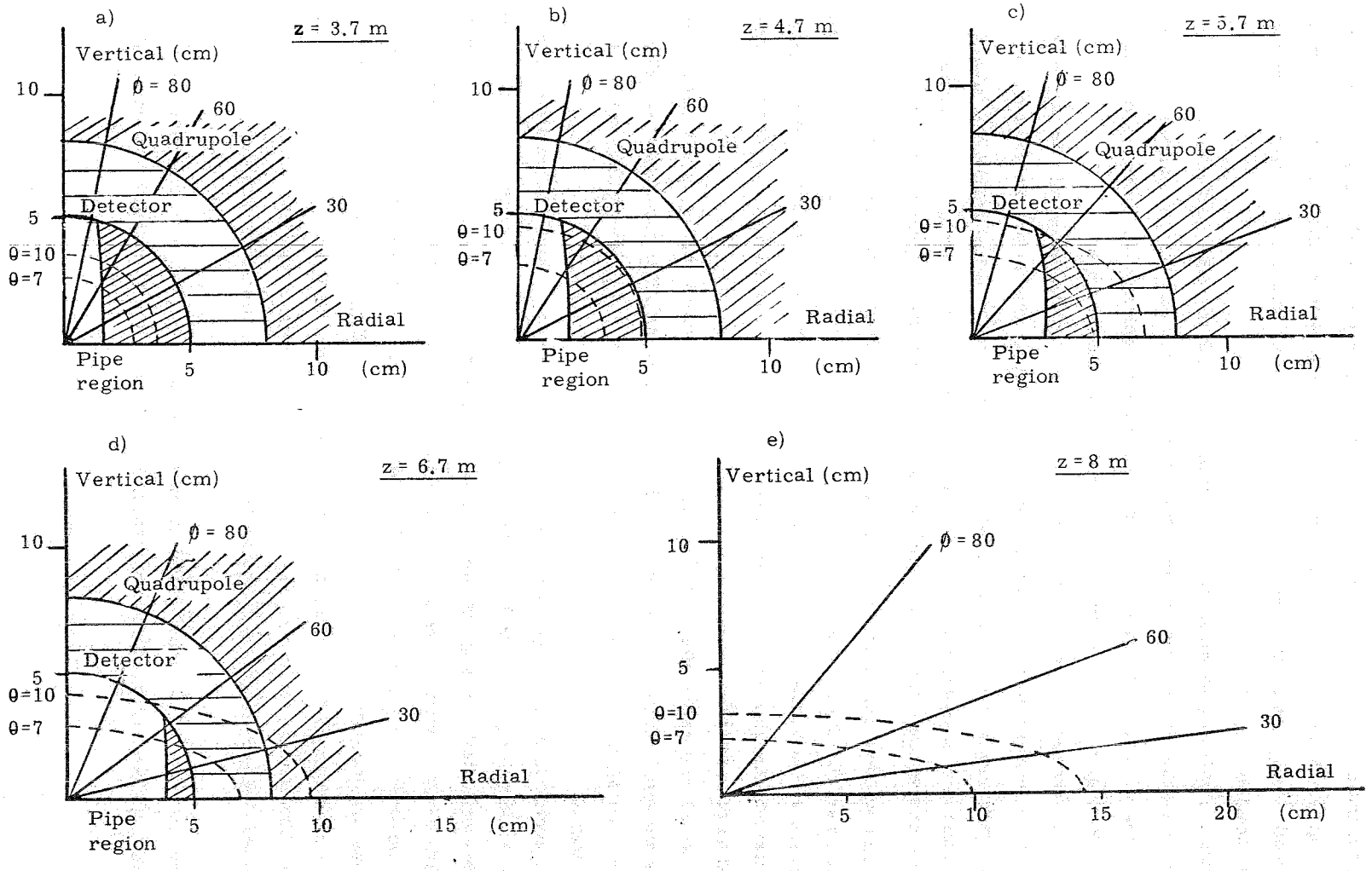

FIG. 6 - Cross sections of the detectable trajectories (case B). The figg. a, b, c, d and e are relative to trasverse planes at z = 3.7, 4.7, 5.7, 6.7 and 8 m.

4. - SYNCHROTRON RADIATION EMITTED IN THE QS1 AND QS2 QUADRUPOLES.

In this Section we investigate on the amount of synchrotron radiation produced by the LEP beam passing through the quadrupoles QS1 and QS2 and falling on the wall of the beam pipe supposed to be 10 cm in diameter. We think of that to be the main source of synchrotron radiation in the QS1 and QS2 region. We have verified that the synchrotron radiation emitted in the second quadrupole QS2" hits the pipe wall considerably far from the region we are interested and in addition we assume that the synchrotron radiation emitted in the quadrupoles Q3, Q4, ... Q9 and in the 10% bending magnet be completely stopped by masks properly disposed upstream on the pipe[7].

The optics of the electron beam in the short insertion causes a synchrotron radiation emission larger in the horizontal than in the vertical plane. That is why we limit ourselves to study the synchrotron radiation emitted only in the horizontal plane.

Since the synchrotron radiation is emitted in a very small cone (at LEP energies of the order of 10 μrad in aperture), one can think with good approximation that the radiation be emitted pratically along the geometrical tangent to the electron trajectory.

Following a typical electron trajectory in the horizontal plane as it is sketched in Fig. 7, one can realize that an electron going into the quadrupole QS2 emits a radiation along a direction, which results progressively bent more and more with respect to the quadrupole axis up to a maximum angle. This maximum angle corresponds to the straight line direction of the electron trajectory between the quadrupole QS1 and QS2'. At the entrance of the QS1 quadrupole the electron radiates again from the maximum angle down to the typical angular values of the beam divergence in the crossing point.

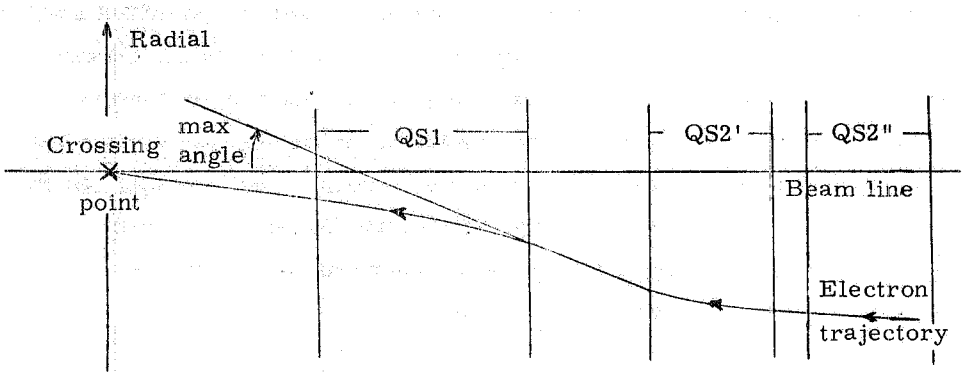

FIG. 7 - Sketch of a typical electron trajectory in the horizontal plane throughout the QS1 and QS2 quadrupoles.

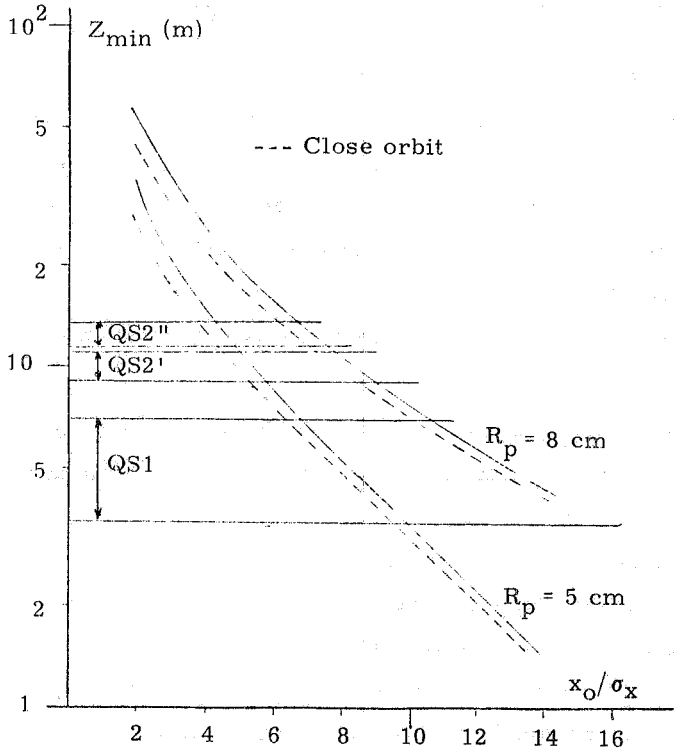

FIG. 8 - Distribution of the minimum value Z_{min} of the pipe wall coordinate corresponding to the nearest point flashed by the synchrotron radiation versus the number of s.d. of the emitting electron. Full lines correspond to the beam pipe diameter of 16 cm and 10 cm. Dashed lines include effects of closed orbit.

In conclusion the synchrotron radiation is emitted from zero to a maximum angle with respect to the quadrupole axis and both quadrupoles contribute to the radiation emitted in this angular range.

Of course the maximum angle is different for different electron trajectories. More an electron is far in the tail of the gaussian spatial distribution of the beam, more its trajectory is large around the equilibrium orbit and more its maximum angle is large.

Let us consider a point on the pipe wall reached by the synchrotron radiation at a distance z from the crossing point, then the minimum value, z_{min}, corresponds to the radiation emitted at the maximum angle.

In Fig. 8 the behaviour of z_{min} is reported versus the number of standard deviation of the gaussian distribution corresponding to the emitting electron. In the figure two full lines correspond to different pipe diameter: 10 cm and 16 cm respectively. Dashed lines include the close orbit effect. In the same figure the regions corresponding to the opposite quadrupoles QS1 and QS2 are also reported. One can see, for instance, that the synchrotron radiation can hit the pipe wall of 10 cm in diameter in the QS1 region only if the radiating electron gets more than 6σ.

We want now evaluate the total synchrotron radiation emitted by the electron beam (I mA at the energy E GeV) and the fraction of this radiation falling on the pipe wall. At this end we need an integration procedure on all possible electron trajectories of the beam.

For this purpose let us consider the parametric equations of the betatron radial oscillation[4] of an arbitrary electron in the crossing point:

$$x = x_o \cos\alpha \,, \qquad x' = x'_o \sin\alpha \,, \tag{3}$$

where x and x' are the canonical variables of the transverse motion and α is a dynamical parameter. In particular in the crossing it can be shown that:

$$x'_o = x_o/\beta^* \tag{4}$$

where β^* is the betatron function. From the equations (3) and the expression (4) one get the equation :

$$x_o^2 = x^2 + \beta^{*2} x'^2 \tag{5}$$

which describes a centered ellipse in the plane (x, x'). Each point of this ellipse represents a possible electron trajectory of a fixed oscillation energy W. In a storage ring beam the energy distribution of the betatron oscillation follows an exponential law :

$$\frac{dN}{dW} = \frac{e^{-W/<W>}}{<W>} \tag{6}$$

and, since the oscillation energy is proportional to the square of the oscillation amplitude, one can deduce from the expression (6) the amplitude distribution law :

$$\frac{dN}{d(x_o/\sigma_x)} = \frac{x_o}{\sigma_x} e^{-\frac{1}{2}(\frac{x_o}{\sigma_x})^2} \tag{7}$$

where σ_x is the gaussian standard deviation.

We define $t = x_o/\sigma_x$ for semplicity sake and perform an integration of the expression (7) at the point t_o in a range $\pm \Delta t$, i. e. :

$$\int_{t_o-\Delta t}^{t_o+\Delta t} t\, e^{-t^2/2}\, dt = 2 \sinh(t_o \cdot \Delta t)\, e^{-\frac{t_o^2+\Delta t^2}{2}} \tag{8}$$

the expression (8) is plotted versus t_o in Fig. 9 for $t_o = n/2$ and $\Delta t = 1/4$ $(n = 1, 2, \ldots, N)$.

By a computing program on each ellipse (corresponding to a given "n") one hundred points have been considered and one hundred corresponding trajectories have been calculated taking the numerical values for $\sigma_x = 0.3$ mm and $\beta^* = 1.6$ m at crossing point. The power radiated in the quadrupoles step by step of length $l = 10$ cm is given by the following expression :

$$\frac{dp}{ds}\, l \int_{t_o-\Delta t}^{t_o+\Delta t} e^{-t^2/2}\, d(t^2/2) \qquad (W) \tag{9}$$

where dp/ds is the power emitted in the length unit :

$$\frac{dp}{ds} = 14.09\, I\, E^4 K^2 y^2 \qquad (W/m) \tag{10}$$

being K the quadrupolar constant (in m^{-2}) and y the distance (in m) of the considered radiating point from the quadrupolar axis.

The total power radiate at each "n" and averaged on the one hundred trajectories is plotted versus $n = x_o/\sigma_x$ in Fig. 10. The values of the beam current and energy used in the expression (10) have been 5.7 mA and 50 GeV respectively. These values correspond to the foreseen phase I of LEP[3].

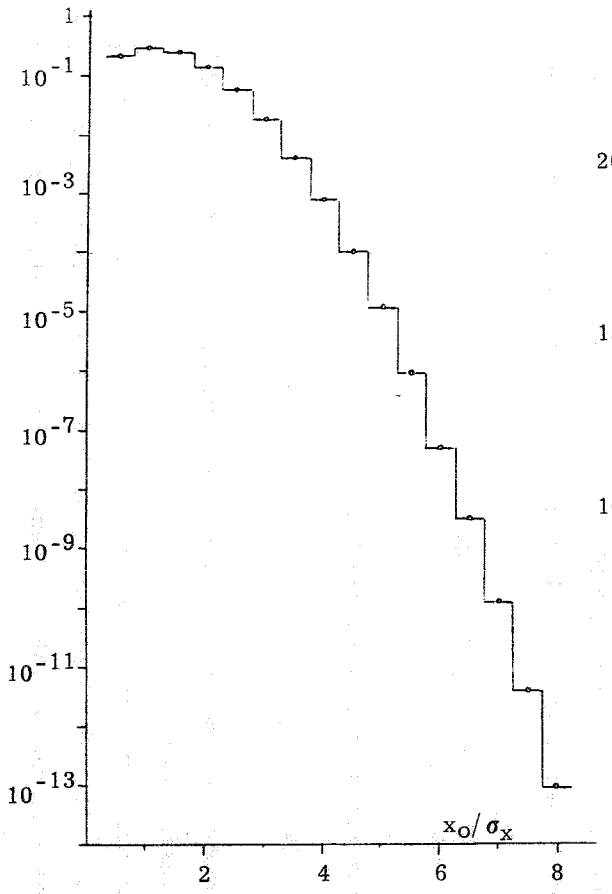

FIG. 9 - Distribution of the betatron oscillation amplitude in the radial direction of the LEP electron beam.

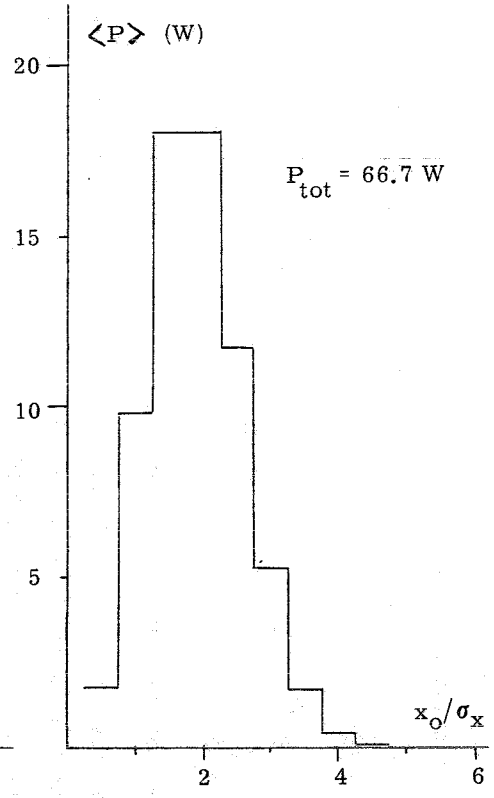

FIG. 10 - Spectrum of the averaged power emitted by electrons of a given number of s.d. of electron beam of 50 GeV in energy and 5.7 mA in current passing through the QS1 and QS2' quadrupoles.

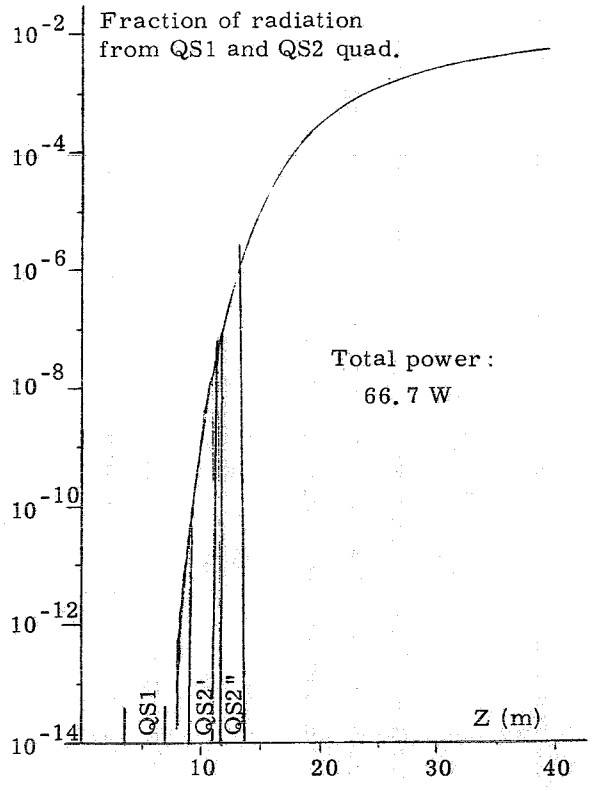

FIG. 11 - Fraction of the total power emitted by the electron beam passing throughout the QS1 and QS2 quadrupoles and falling on the pipe wall of coordinate z (the pipe diameter is 10 cm and beam energy is 50 GeV).

In this way one can get along the pipe coordinate the distribution of the fraction of the total emitted power from QS1 and QS2' quadrupoles. This distribution is shown in Fig. 11. One can see that a level of 6.7×10^{-13} W (equivalent to 4.2 MeV/sec or 0.1 keV/bunch) is starting from $z = 8$ m in the middle of the quadrupole QS1 and QS2'.

In the limits of our approximations we can conclude that no serious synchrotron radiation background is present in the QS1 region and that a total energy absorption electron counter located inside the quadrupole QS1 is safe by the synchrotron radiation generated into the opposite quadrupoles QS1 and QS2'.

5. - REAL ELECTRON BEAM EFFECT ON THE BHABHA SCATTERING RATE.

The results reported so far refer to an ideal electron beam, that means a zero emittance beam and no close orbit effects. In this Section we want to look at the effects of a real beam on the Bhabha scattering rate. We describe the real beam as it is shown in Table II, where the spatial and angular deviations are reported both for the statistical deviations (see ref. (3)) and systematical ones coming from recent calculations[5].

TABLE II - LEP beam spatial and angular deviations in the short insertion.

Error	Spatial (mm)		Angular (mrad)	
	vertical	radial	vertical	radial
Systematic	1	1	0.3	0.1
Statistic	0.017	0.37	0.17	0.23
	0.065[x]		0.65[x]	

[x] Full coupling

In order to value the effect of the real beam on the Bhabha rate, we refer to a work[2] we did in the LEP Study Group activity on the tagging efficiencies at the short insertion. In that work we have shown that if the incident direction of the electrons is changed by a deviation angle $\alpha \neq 0$, the corresponding "detected trajectories fraction" spectra are modified in some way with respect to the $\alpha = 0$ case. In particular for a vertical beam deviation no change is expected in the small angle region of the spectrum. Since the Bhabha rate depends strongly on the accepted minimum angle, we can limit our analysis only to the radial angular deviation. In addition we can also neglect the spatial deviations of the beam, because they produce an effect smaller than that of the angular deviation.

The results of our calculations show that, when an angular beam deviation is present, the "detectable trajectories fraction" spectrum is always modified in such a way that the small angle threshold is lowered. Therefore the Bhabha rate becomes a little larger than that relative to an ideal beam. The results we have obtained on the statistical angular distribution of the beam show an increase of the Bhabha rate of 1.2%, the systematic part an increase of 0.5%.

6. - OFF MOMENTUM PARTICLES BACKGROUND.

The rate of the luminosity monitor is certainly contaminated by the off momentum particles coming from the beam-gas bremsstrahlung. The level of this background depends on many parameters, like the vacuum distribution inside the pipe, the background configuration with respect to the monitor position, tha background energy spectrum with respect to the energy resolution of the monitor and so on.

In this Section we can give only a rough estimation of this background for the lay-out shown in Fig. 1, since the available informations[6, 7] on this subject in the literature refer to the short insertion configuration as given in the "Pink Book" design. We refer to the phase I of LEP (E = 50 GeV, I = 5.7 mA) and to a luminosity of $4 \times 10^{31}\ cm^{-2}\ sec^{-1}$ as given in ref.(3).

We suppose that the two arms of the luminosity monitor be composite by an inner and outer part (with respect to the machine centre) and be capable of measuring the electron energy with a resolution of the order of 20%.

In the region between the quadrupole QS1 and QS2 we suppose a flux of the off momentum particles of 1.5×10^{-3}/bunch/m in the energy range from 40 to 50 GeV[6]. The probability of an accidental event on the coincidence of the two arms turns out to be 5×10^{-6}/bunch.

For the region inside the quadrupole QS1 we haven't any precise information on the off momentum particles background. However taking the same flux per bunch and per length unit (perhaps optimistic) we find for the monitor inside quadrupole a probability of accidental event of 10^{-4}/bunch. That means that in the above mentioned conditions the expected rates are:

for case A	Bhabha events	34 ev/s
	accidentals	0.2 ev/s
	ratio	0.005 acc/Bh.

for case B

- using the whole length of counter ($\sim$ 4 m)

	Bhabha events	120 ev/s
	accidentals	4 ev/s
	ratio	0.033 acc/Bh

- using only 1 m of counter (grated part of Fig. 1b)

	Bhabha events	120 ev/s
	accidentals	0.2 ev/s
	ratio	0.002 acc/Bh.

ACKNOWLEDGEMENTS.

We want to thank K. Potter and A. Smith for their clever collaboration in dealing problems of experiment-machine matching. We appreciate the kindness of T. Taylor in providing us necessary data on the mini-beta lattice. We thank our friends of the ADONE machine group S. Tazzari, M. Preger and M. Bassetti for many illuminating discussions.

REFERENCES.

(1) - P. Strolin, Summary and conclusions on the experimental areas, background and isertion, in Proceedings of the General Meeting on LEP, Villars-on-Ollon, June 1981.

(2) - R. Del Fabbro and G. P. Murtas, Tagging system at LEP short insertion: angular acceptances and efficiencies, Frascati report LNF-79/23 (1979); Two photon mass sensitivity by a tagging system at LEP short insertion, Frascati report LNF-79/40 (1979).

(3) - Design study of a 22 to 130 GeV e^+e^- colliding beams machine (LEP), CERN (1979) (Pink Book).

(4) - See for instance the M. Sand's paper: The physics of electron storage rings, An introduction, Stanford Report SLAC-121 (1970).

(5) - M. Bassetti, private communication.

(6) - A. Smith, Off momentum particles producing background in LEP 8, LEP note 164 (1979).

(7) - K. Potter, Background prospects at LEP, in Proceedings of the General Meeting on LEP, Villars-on-Ollon, June 1981.